ACS Catalysis

Research Article

pubs.acs.org/acscatalysis

Supported Pd Catalysts Prepared via Colloidal Method: The Effect of Acids

Yingnan Zhao,[†,‡] Lijun Jia,[‡,§] José A. Medrano,[†] Julian R. H. Ross,[§] and Leon Lefferts*[,†]

[†]Catalytic Processes and Materials, MESA+ Institute for Nanotechnology, University of Twente, Enschede, 7500AE, The Netherlands

[‡]School of Chemical Engineering, Tianjin University, Tianjin 300072, China

[§]Chemical & Environmental Sciences Department, University of Limerick, Limerick, Ireland

Supporting Information

ABSTRACT: Organic capping agents are necessary for metallic nanoparticle preparation via colloidal method; however, complete removal of the capping agent and cleaning the metal surface is a well-known challenge in application. In this Article, we show that polyvinyl alcohol (PVA)-stabilized palladium nanoparticles (Pd NPs) were prepared and immobilized on activated carbon (AC). Different acids (HCl and H_2SO_4) were used to adjust the pH, thus enhancing the adsorption of the colloid on the support. The catalysts were characterized by TEM, CO-chemisorption, XRF, N_2 physisorption, XPS, TGA, and temperature-programmed reduction MS. Activity of the catalyst was tested using nitrite hydrogenation in aqueous phase and formic acid decomposition in gas phase as probe reactions. The results showed that chlorine, introduced via HCl, efficiently suppressed the interaction of the Pd NPs with PVA. Clean Pd NPs were obtained without any significant sintering after reduction in H_2/N_2 at mild temperature (200 °C). The influence of acid on PVA thermal stability was also investigated. Differences in catalytic activity in gas phase versus liquid aqueous phase indicated that the extent of PVA covering the Pd NPs is phase-dependent.

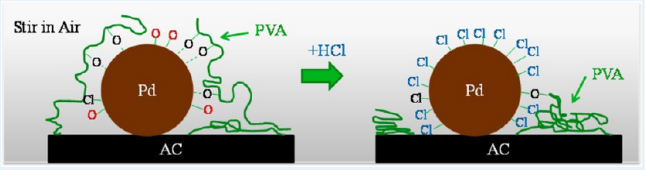

KEYWORDS: *PVA capping, Pd colloid, activated carbon, chlorine, thermal treatment*

1. INTRODUCTION

Colloid immobilization has been widely used to prepare nanoparticles (NPs) for catalytic applications. Many benefits have been reported regarding this method: namely, accurate control over particle size and shape as well as a result of highly active and selective catalysts as compared with catalysts prepared via traditional methods (e.g., impregnation).[1−4] Capping agents such as long-carbon-chain compounds, surfactants, and organic ligands are commonly used as stabilizers to prepare colloids. The nanoparticle size and shape can be manipulated by altering the chain length of the capping agent, nature of the associated counterion, concentration, and affinity toward specific crystal facets.[5] However, the capping agent can also constitute a protective layer, which in many cases limits the accessibility of the active sites for the reactants in both gas and liquid phase operation.[3,6,7] Therefore, the capping agent on the NPs should be removed as completely as possible.

Capping agent removal has been developed following several approaches involving oxidation or thermal treatment. Aliaga et al. proposed treatment by UV−ozone to remove organic capping agents from Pt nanoparticles deposited on silicon wafers.[8] For colloids immobilized on porous support materials, thermal treatments in oxidative, inert or reductive atmosphere are widely used at temperatures above 300 °C to remove the capping agent. High temperature and exothermal procedures, however, can result in a significant change in the nanoparticle size via agglomeration, especially for monometallic Pd NPs.[4,9−11] Furthermore, any remaining carbonaceous deposits after thermal treatment might affect the catalytic performance.[12] Recently, Lopez-Sanchez et al. established a new approach to partially remove capping polyvinyl alcohol (PVA) from Au and Au/Pd alloy immobilized on TiO_2 via refluxing the catalyst slurry in water at 90 °C.[13] However, this approach would not be applicable in the case of weak interaction of the colloid particles with the support (e.g., on activated carbon (AC)), resulting in metal loss during refluxing. Furthermore, weak interaction between Pd NPs and the support implies relatively poor protection against sintering[14] so that mild temperatures during any treatment become even more critical.

In this Article, we show that Pd NPs with narrow particle size distribution supported on AC were prepared via colloidal immobilization using PVA as capping agent. During the immobilization, acid (usually sulfuric acid, H_2SO_4) needs to be added to adjust the pH to enhance adsorption of the colloid on the support material. This study reports on an unexpected effect of the type of acid—H_2SO_4 versus HCl—on the accessibility of the Pd NPs.

Received: June 13, 2013
Revised: August 29, 2013
Published: September 2, 2013

   dx.doi.org/10.1021/cs4004479 | ACS Catal. 2013, 3, 2341−2352

2. EXPERIMENTAL SECTION

2.1. Chemicals. Sodium tetrachloropalladate(II) (Na_2PdCl_4 ≥ 99.995% (metal basis)), polyvinyl alcohol (PVA, average MW = 13 000−23 000, 87−89% hydrolyzed), sodium borohydride ($NaBH_4$, ≥ 96% (gas-volumetric)), and formic acid (98−100%) were purchased from Sigma-Aldrich. Sodium nitrite (>99%) was purchased from Merck. Activated carbon (AC, SX Ultra 94031-8, S_{BET} = 1100 $m^2\ g^{-1}$) was supplied by Norit, and sieved in the range of 38−45 μm in diameter. All the aqueous solutions were prepared using ultrapurified water obtained on a water purification system (Millipore, Synergy).

2.2. Pd Nanoparticle Synthesis. Pd NPs were synthesized according to a method described in the literature,[15] which can be summarized as follows: PVA was dissolved in water at 70 °C with stirring for at least 2 h. The solution (2 wt %) was then cooled to room temperature. An aqueous solution of Na_2PdCl_4 (20 mL, containing 0.086 mmol Pd) and 1.76 mL of freshly prepared PVA solution were added to 240 mL water, obtaining a yellow-brown solution. After 3 min, $NaBH_4$ solution (1.72 mL, 0.172 mmol) was added under vigorous stirring. The brown Pd colloid solution was immediately formed. The final pH was typically 8−8.5.

2.3. Catalyst Preparation. *Preparation of 1 wt % Pd Supported on Activated Carbon.* Activated carbon (0.75 g) was added to the Pd colloid solution (260 mL, 3.3×10^{-4} mol L^{-1}) immediately after preparation. A solution of acid, either hydrochloric or sulfuric, was added to adjust the pH to 2. The slurry was agitated, exposed to air, for 2 h at room temperature; filtered; and thoroughly washed with water. After that, the catalysts were dried in vacuum at 40 °C overnight.

Thermal Treatment. Catalysts prepared using different acids were carefully treated in a tube furnace. In a typical procedure, the temperature was raised to 200 °C at a rate of 5 °C min^{-1}, then kept for 1 h at 200 °C in 10 vol % H_2/90 vol % N_2. Then the sample was flushed in N_2 for 30 min at 200 °C and cooled at a rate of 20 °C min^{-1} to room temperature in the same atmosphere. The catalysts were flushed in N_2 for 24 h before exposure to air. In the following, the sample notation will be used as shown in Table 1.

2.4. Characterization. Pd particle size distribution was determined using TEM (Philips CM300ST-FEG) with a resolution of 1 nm. The AC-supported catalysts were first ground into submicrometer fragments and dispersed in ethanol, then the suspension was dropped on a copper grid covered with hollow carbon for TEM image taking. At least five of these ground fragments were randomly selected for determination of Pd particle sizes, and typically, 300 Pd particles were measured. Note that information on the spatial distribution of nanoparticles through the support cannot be obtained. The metal loadings on the supports were analyzed by XRF. The total surface areas of the samples were calculated on the basis of the N_2 physisorption data, using the BET method for p/p_0 values between 0.03 and 0.13 following the recommendations of Rouquerol et al.,[16] with a typical margin of error of 5%.

CO chemisorption at room temperature was used to determine the metal surface area that is accessible in the gas phase. Typically, the sample was prereduced at 100 °C in hydrogen and then flushed in He at the same temperature. After cooling, CO was introduced as pulses, and the response was recorded using a TCD detector. We assumed that the stoichiometric ratio of the number of adsorbed CO molecules and number of accessible Pd surface atoms is 1:1. The Pd dispersion (Pd disp) was defined as

$$\text{Pd disp} = \frac{\text{number of Pd atoms in the surface of NPs}}{\text{number of Pd atoms in total}}$$

The surface of the catalysts was analyzed by X-ray photoelectron spectroscopy (XPS, Quantera SXM, Al Kα (1486.6 eV)). The powder samples were stored in air without any further pretreatment before analysis. Typically, a few microgram sample was pressed into an indium foil, and four spots (600 × 300 μm^2) on the sample were randomly selected for measurement to rule out the inhomogeneity in the catalysts. The accuracy of the resulting peak positions was within 0.2 eV. The spectra were fitted using the software Multipak v.9.4.0.7. Typically, the banding energy in all spectra was first calibrated using the carbon 1s peak at 284.8 eV as an internal reference. The spectra detected from the four spots of one sample were averaged to improve the signal-to-noise ratio, followed by Shirley background subtraction. The Pd peaks were fitted using an asymmetric model, caused by interaction of the photoelectron with valence band electrons,[17] whereas the S and Cl peaks were fitted using a mixed Gaussian−Lorentzian model, as suggested by the *Handbook of X-ray Photoelectron Spectroscopy*.[18] The peaks for each sample (Pd 5d, Cl 2p, and S 2p) were fitted with sets of doublets with identical FWHM. Both width and peak position were allowed to optimize. The distance within the doublets was fixed with the data suggested in the handbook.[18]

Thermal gravimetric analysis (TGA) was performed in either Ar or 10 vol % H_2/90 vol % Ar (flow rate 50 mL min^{-1}). The sample was first heated to 70 °C and kept at this temperature for 1 h to remove the major part of the water, then the temperature was increased from 70 to 600 °C at a rate of 5 °C min^{-1}. The weight change was calculated on the basis of the weight of the dried sample at 70 °C.

Temperature-programmed reduction/desorption (TPR or TPD) analyses were carried out using a home-built setup. The sample was first flushed in Ar at 70 °C for 1 h and then cooled to room temperature. TPR and TPD were performed using 20 mL min^{-1} flow of 5% H_2/95% Ar or pure Ar, respectively, and using a heating rate of 5 °C min^{-1}. Mass spectrometry was used to analyze qualitatively the composition of the resulting gas stream.

2.5. Catalytic Activity. *2.5.1. Formic Acid Decomposition in the Gas Phase.* The activity of catalysts for formic acid catalytic decomposition (Scheme 1) was determined in a home-

Table 1. Sample Notations and Details of Corresponding Preparation Procedure[a]

sample	preparation procedure
PVA/AC_Cl	AC impregnated with PVA solution using HCl to adjust pH to 2
PVA/AC_S	AC impregnated with PVA solution using H_2SO_4 to adjust pH to 2
Pd-PVA/AC_Cl	Pd-PVA colloid immobilized on AC using HCl to adjust pH to 2
Pd-PVA/AC_Cl_H	Pd-PVA/AC_Cl treated in H_2/N_2 at 200 °C for 1 h
Pd-PVA/AC_Cl_N	Pd-PVA/AC_Cl treated in N_2 at 200 °C for 1 h
Pd-PVA/AC_S	Pd-PVA colloid immobilized on AC using H_2SO_4 to adjust pH to 2
Pd-PVA/AC_S_H	Pd-PVA/AC_S treated in H_2/N_2 at 200 °C for 1 h

[a]Note that the first two samples do not contain Pd.

Scheme 1. Formic Acid Decomposition

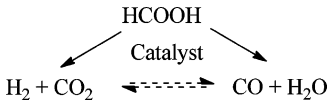

built, continuously operated, fixed-bed reactor.[19] Typically, 50 mg of catalyst was loaded in a fixed-bed quartz tubular reactor (4 mm in diameter). The catalyst was first rereduced in a 1 vol % H_2/Ar mixture for 1 h at 25 °C to remove adsorbed oxygen introduced during storage in air, then a stream of He was passed through a formic acid trap before being introduced into the reactor. The typical feeding concentration of formic acid in the gas phase was 2.0 vol %. The total flow rate of the gas mixture was 51 mL min^{-1}. The reaction was performed at 120 °C in steady state. The concentrations of formic acid and products were determined by gas chromatography. The conversion of formic acid was kept below 20%.

The activity per total amount of Pd in the catalyst (mol_{HCOOH} mol_{Pd}^{-1} min^{-1}) was defined as

$$R_{W,HCOOH} = -\frac{C_{HCOOH} - C_{HCOOH,0}}{W/F_{HCOOH}}$$

where C_{HCOOH} is the formic acid concentration (mol L^{-1})), $C_{HCOOH,0}$ is the feeding formic acid concentration (mol L^{-1}), W is the total moles of Pd atoms (mol), and F_{HCOOH} is the feeding flow rate of formic acid (L min^{-1}).

Alternatively, assuming identical accessibility of the Pd surface sites for chemisorbed CO and formic acid in gas phase, the activity can also be expressed as per accessible Pd surface sites (mol_{HCOOH} mol_{Pd}^{-1} min^{-1}),

$$R_{S,HCOOH} = -\frac{C_{HCOOH} - C_{HCOOH,0}}{S/F_{HCOOH}}$$

where S is defined as the amount of accessible Pd based on CO chemisorption in the gas phase (mol).

$$S = W \times \text{Pd disp}$$

2.5.2. Nitrite Hydrogenation in Liquid Phase. The activity of the catalysts for nitrite hydrogenation (eq 1 and 2) was determined in a continuously operated fixed-bed reactor made of PEEK. Typically, 40 mg of catalyst powder was packed in a 4-mm-diameter reactor, resulting in a bed height of ~10 mm. The feed stream contained 515 μmol L^{-1} (23.7 $mg_{nitrite}$ L^{-1}) sodium nitrite and 432 μmol L^{-1} hydrogen in water. The hydrogen concentration was obtained by saturating the solution with 60 vol % H_2/Ar at 1 bar. In this way, the catalyst is contacted with aqueous solution only and no gas phase is present in the reactor, excluding any effects of gas–liquid transfer on the kinetic data obtained. The flow was set at 3.5 mL min^{-1} using an HPLC pump (Dionex, Ultimate 3000), resulting in space time τ = 28 min^{-1} (τ = (flow rate)/(catalyst bed volume)) and a pressure drop of typically 1 bar. Nitrite concentrations were measured by ion chromatography (Dionex, ICS 1000) by injecting a 25 μL sample of the liquid stream leaving the reactor through a six-port valve. The reaction was performed under differential conditions, keeping the conversion of nitrite at ~5%.

$$2NO_2^- + 3H_2 + 2H^+ \xrightarrow{Pd} N_2 + 3H_2O \quad (1)$$

$$NO_2^- + 3H_2 + 2H^+ \xrightarrow{Pd} NH_4^+ + 2H_2O \quad (2)$$

The activity per total amount of Pd in the catalyst ($mol_{nitrite}$ mol_{Pd}^{-1} min^{-1}) was defined as

$$R_{W,nitrite} = -\frac{C_{nitrite} - C_{nitrite,0}}{W/F_{nitrite}}$$

where $C_{nitirite}$ is the nitrite concentration (μmol L^{-1}), $C_{nitirite,\ 0}$ is the initial nitrite concentration (μmol L^{-1}), and $F_{nitrite}$ is the flow rate (L min^{-1}).

Alternatively, assuming identical accessibility of the Pd surface sites in both the gas and liquid phases, the activity can also be expressed as per accessible Pd surface sites ($mol_{nitrite}$ mol_{Pd}^{-1} min^{-1}):

$$R_{S,nitrite} = -\frac{C_{nitrite} - C_{nitrite,0}}{S/F_{nitrite}}$$

Table 2. Summary of XRF Elemental Analysis, CO Chemisorption, and TEM

sample	treatment	C_{Cl} (wt %)	C_S (wt %)	particle size[a] (nm)	Pd disp (%)	
					TEM	CO chem[c]
AC		0.13 ± 0.01				
AC_Cl		1.0 ± 0.1				
PVA-AC_Cl		0.85 ± 0.08				
	H_2/N_2, 200 °C	0.34 ± 0.03				
	N_2, 200 °C	0.35 ± 0.03				
PVA-AC_S		0.04 ± 0.01	0.71 ± 0.07			
Pd-PVA/AC_Cl		1.4 ± 0.1		2.8 ± 0.8	38	6[b]
	H_2/N_2, 100 °C	0.85 ± 0.08				31
	H_2/N_2, 200 °C	0.16 ± 0.02		3.0 ± 0.9	35	36
	N_2, 200 °C	1.1 ± 0.1		3.0 ± 0.8	35	8[b]
Pd-PVA/AC_S		0.54 ± 0.05	0.44 ± 0.02	2.9 ± 0.9	36	4[b]
	H_2/N_2, 100 °C					10
	H_2/N_2, 200 °C	0.08 ± 0.01	0.42 ± 0.02	3.0 ± 0.8	35	17
	H_2/N_2, 250 °C			3.1 ± 1.0	34	22

[a]Observed in TEM. [b]The sample was reduced at room temperature for 1 h before CO chemisorption, which is known to be sufficient for removal of adsorbed oxygen from Pd catalyst.[20,21] [c]Please note that apparent Pd dispersions were obtained by CO chemisorption, because part of the Pd surface was not accessible for CO bedcause of PVA blocking and Cl poison, as discussed below.

dx.doi.org/10.1021/cs4004479 | ACS Catal. 2013, 3, 2341–2352

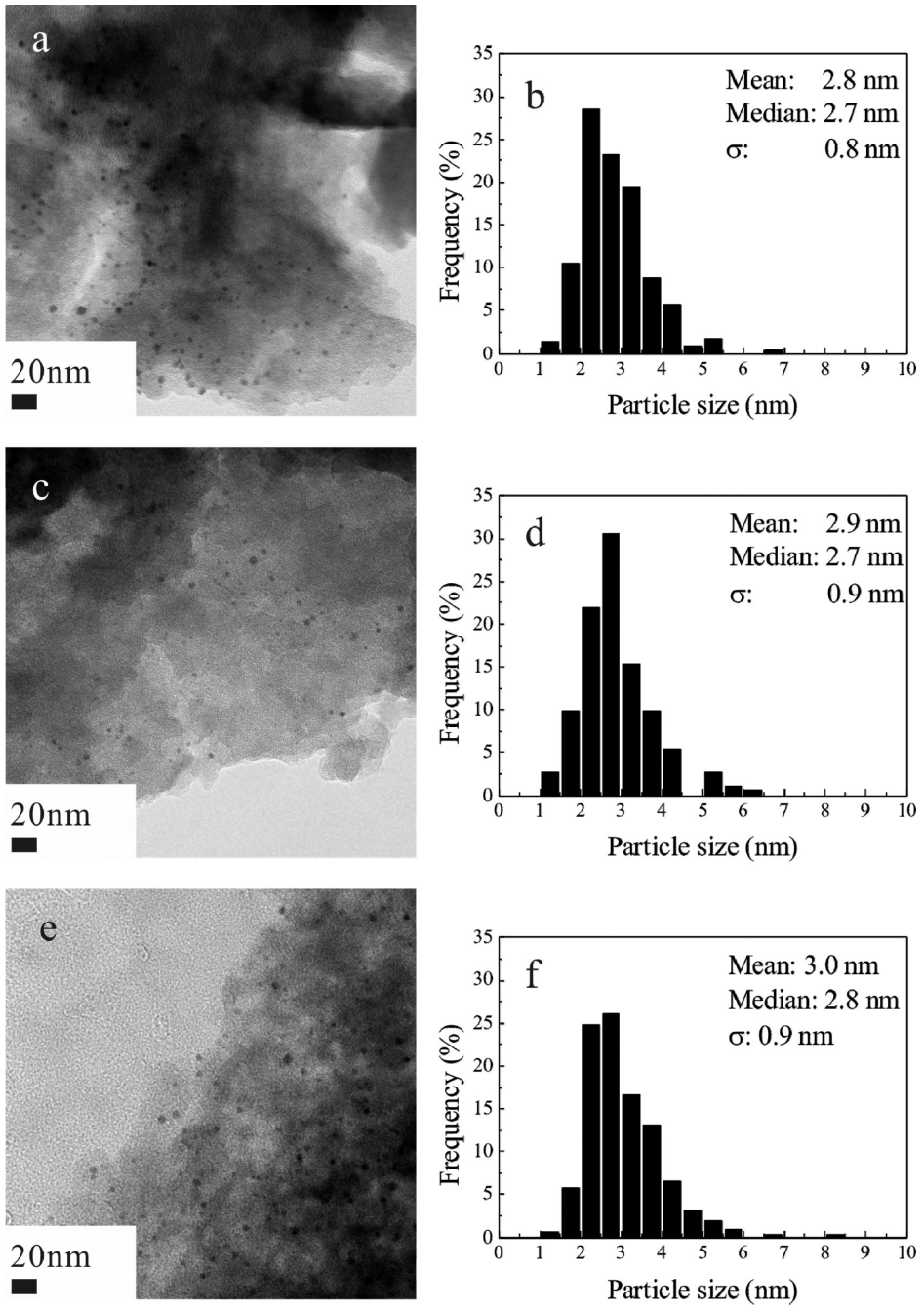

Figure 1. TEM image and corresponding Pd particle size distribution of Pd-PVA/AC_Cl (a and b), Pd-PVA/AC_S (c and d), and Pd-PVA/AC_Cl_H (e and f).

3. RESULTS

3.1. Elemental Analysis. The Pd, Cl, and S loadings were measured with XRF. All catalysts had the same Pd loading of 1.1 wt %. As shown in Table 2, the commercial AC support contained a minor amount of chlorine, as low as 0.13 wt %. After using HCl to adjust the pH of the aqueous slurry and stirring for 2 h, the chlorine loadings increased to about 1.0 wt %, and the absence or presence of PVA had no significant effect. Interestingly, when H_2SO_4 was used to impregnate PVA onto AC, the chlorine loading was even lower than that in the original AC. For as-prepared Pd catalyst using HCl, the loading of chlorine was as high as 1.4 wt % and was decreased to 0.85 wt % after reduction in H_2/N_2 at 100 °C, decreasing even further to 0.16 wt % after reduction at 200 °C. Thermal treatment in N_2 at 200 °C caused removal of only a minor fraction of the chlorine, to 1.1 wt %. Correspondingly, when H_2SO_4 was used, the chlorine loading decreased from 0.54 to 0.08 wt % after reduction in H_2/N_2 at 200 °C. The sulfur content in the original AC was negligible. When PVA was impregnated on AC using H_2SO_4, the sulfur content increased to 0.71 wt %. Unlike chlorine, the sulfur loading was not significantly increased by the presence of Pd.

3.2. Pd Particle Size. Figure 1 shows a narrow particle size distribution in as-prepared catalysts according to TEM. The mean particle size of the catalyst prepared with HCl was 2.8 nm and was very similar to that of catalyst prepared using H_2SO_4 (2.9 nm). An example of the particle size distribution in

dx.doi.org/10.1021/cs4004479 | ACS Catal. 2013, 3, 2341−2352

thermally treated catalysts is shown in Figure 1e and f, showing that the particle size remained in the range of 3 nm after thermal treatment in H_2/N_2 or in N_2 at 200 °C. The particle size distributions were not significantly influenced by any of the thermal treatments, as shown in Table 2. All the nanoparticles were spherical as observed with TEM, as shown in Figure 1 and Supporting Information Figure S3.

3.3. CO Chemisorption. CO chemisorption was used to determine the accessibility of Pd atoms in the gas phase. As shown in Table 2, the apparent Pd dispersions of these samples were quite different according to CO chemisorption, although the particle sizes and Pd loadings were almost the same for all samples. According to CO chemisorption, the apparent Pd dispersion was as low as 6% for as-prepared catalyst prepared using HCl; this apparent dispersion increased to 31% and further to 36% after reduction at 100 and 200 °C, respectively, in H_2/N_2 atmosphere. However, thermal treatment in N_2 did not significantly change the apparent Pd dispersion (8%).

The as-prepared catalyst prepared using H_2SO_4 also showed a low apparent Pd dispersion of 4%. After reduction at 100 °C, the apparent Pd dispersion was still as low as 10%, and it increased to 17% and further to 22% as the result of reduction at 200 and 250 °C in H_2/N_2, respectively.

3.4. Porosity. Both the total surface area and the surface area of the micropores (<2 nm) were calculated on the basis of N_2 physisorption isotherms. Figure 2 shows the effect of PVA,

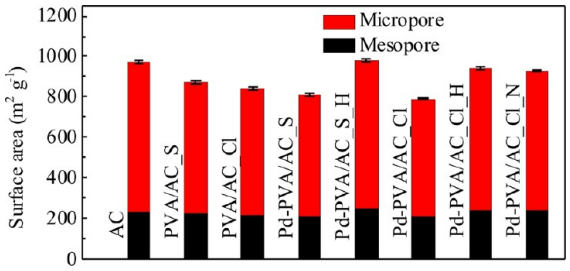

Figure 2. Surface area of micro- and mesopores. The surface area of micropores was calculated by the *t*-plot method using data of N_2 physical adsorption. The mesopore surface area was estimated on the basis of the difference between the BET surface area and the micropore surface area.

including various pretreatments, on the surface area of both the micropores and mesopores. Micropore surface areas decreased in the order AC > PVA/AC_S > PVA/AC_Cl > Pd-PVA/AC_S > Pd-PVA/AC_Cl. After the thermal treatments, micropore surface areas of the catalysts increased to values similar to the original AC. In contrast, the effect of PVA on the surface area of mesopores was not significant within the experimental error.

3.5. XPS. Figure 3a shows the effect of thermal treatments of catalyst prepared with HCl on the oxidation state of Pd according XPS. Table 3 presents the full data set of peak positions resulting from the fitting procedure as well as the ratio values for Pd^{2+}/Pd^0, showing that the as-prepared catalyst contained 38% Pd^{2+}. Thermal treatment in H_2/N_2 at 100 and 200 °C resulted in partial and almost complete reduction, respectively, as shown in Table 3b. Interestingly, the thermal treatment in inert atmosphere at 200 °C also partially reduced oxidized Pd, as shown in Figure 3a and Table 3b. Table 3b also shows that in as-prepared catalyst using H_2SO_4, the Pd^{2+} content was significantly lower as compared with the catalyst prepared using HCl. Similarly, in the case of using HCl, thermal treatment in H_2/N_2 at 100 and 200 °C resulted in partial and almost complete reduction, respectively; however, thermal treatment in inert atmosphere did not influence the amount of oxidized Pd significantly, in contrast to the catalyst prepared with HCl.

Catalyst prepared using HCl contained two types of chlorine with formal charge Cl^-, as shown in Figure 3c and Table 3a, which can be attributed to Cl bonded to Pd (~198 eV) and Cl in organic compounds (~200 eV), respectively.[22] After thermal treatments at 200 °C in either H_2/N_2 or N_2, the relative amount of Cl bonded to carbon increased (Table 3b).

Sulfur in as-prepared Pd-PVA/AC_S is mainly observed as S^{6+}, as shown in Figure 3b, indicating the presence of sulfate, sulfonic acid or sulfone species.[23] Thermal treatment in H_2/N_2 results in reduction of S^{6+} to 0 or negatively charged sulfur species, typically elemental sulfur, sulfide, disulfide, thiol, or thiophene,[23,24] especially at higher temperature, as shown in Table 3b.

3.6. TGA-DTG study. TGA was used to study desorption and decomposition of PVA. Figure 4a, b, and c shows TGA-DTG results in an Ar atmosphere of the original commercial AC and AC treated with HCl or H_2SO_4, respectively. Table 4 summarizes the results in terms of peak position and weight loss at 200 °C, showing weight loss in the same temperature window for the original AC and AC treated in HCl solution (pH = 2). However, the sample treated in HCl lost much more weight (1.62 wt %) as compared with the original AC (0.34 wt %). This difference might be due to desorption of HCl. The AC treated in H_2SO_4 showed hardly any desorption below 160 °C; instead, a clear weight loss was observed around 240 °C. The presence of H_2, instead of Ar only had no influence on any of these experimental results, as shown in Table 4.

As shown in Figure 4d, a mechanical mixture of PVA and AC showed mainly weight loss around 340 °C, similar to results obtained with PVA only (data not shown). The products detected in the gas phase, as indicated in Table 4, included H_2O, CO_2, and the $-CH_3$ fragment (m/z = 18, 44, and 15, respectively). The presence of the CO_2 and $-CH_3$ fragment can be attributed to the formation of carboxyl acids as decomposition product originating from acetyl groups in PVA (87−89% hydrolyzed).[25] The $-CH_3$ fragment observed at 400 °C, however, indicates an alternative decomposition pathway of PVA.[26]

The stability of PVA on AC was strongly affected by the acid (H_2SO_4 or HCl) used during colloid immobilization. As shown in Figure 4e, PVA/AC_S showed a major weight loss at a significantly lower temperature, around 190 °C. The compounds produced were identical to those observed with PVA only according to MS (Table 4). Therefore, these products were likely to originate from PVA decomposition. When HCl was used instead, four weight loss steps were observed, as shown in Figure 4f. The weight loss at 120 °C was due to physically adsorbed H_2O or HCl, similar to what was observed on the HCl-treated AC. The two following weight loss steps at 315 and 400 °C were similar to the decomposition pattern of PVA (not shown) as well as the PVA and AC mechanical mixture (Figure 4d). In addition, the products detected in the gas phase were identical (Table 4). In addition, a new weight loss step appeared around 250 °C, as shown in Figure 4d and Table 4. The volatile products detected were again similar to PVA decomposition. It should be noted that HCl was never detected with MS; however, it cannot be ruled out that any

dx.doi.org/10.1021/cs4004479 | ACS Catal. 2013, 3, 2341−2352

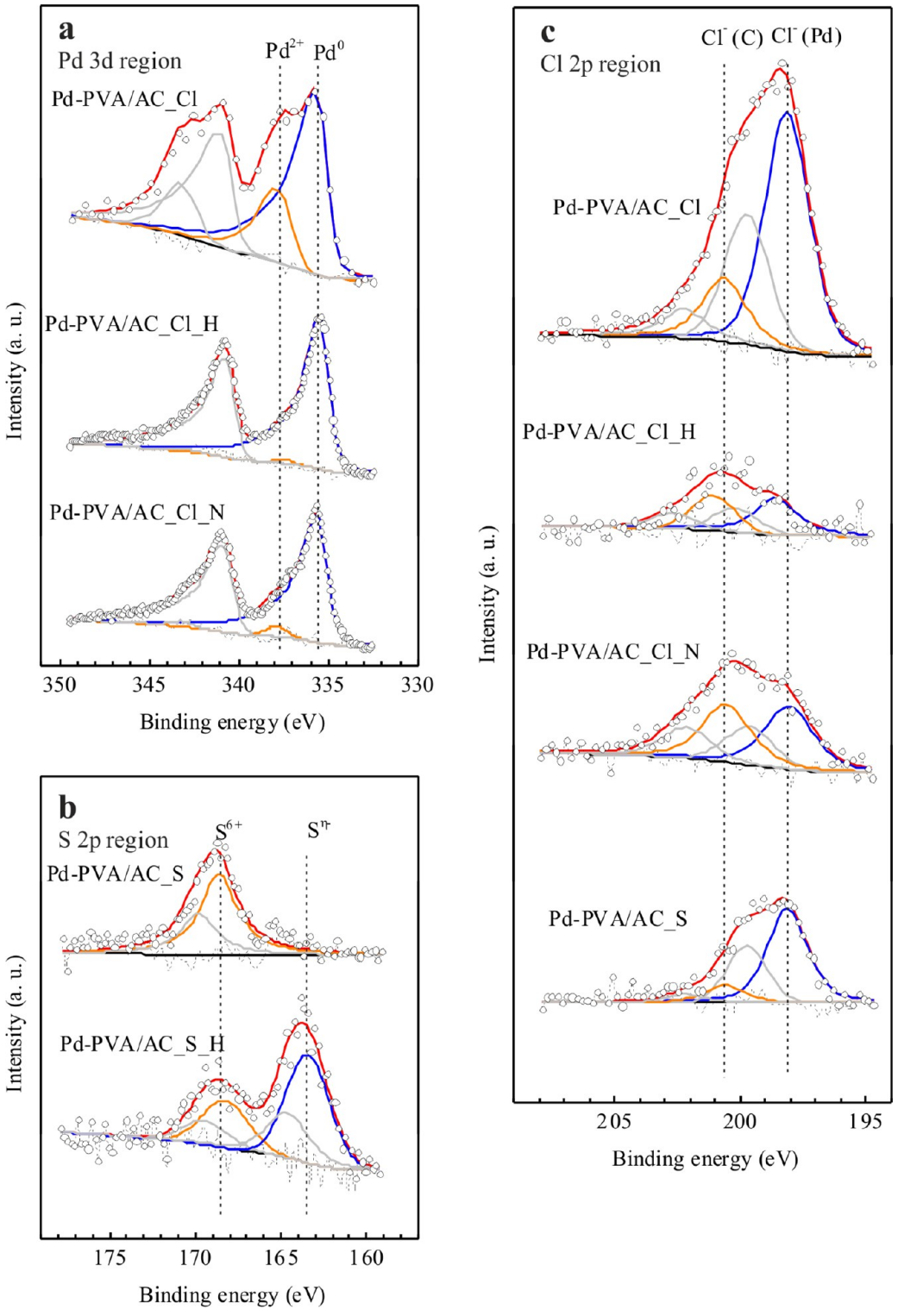

Figure 3. XPS spectra of activated carbon supported Pd-PVA colloids: (a) Pd 3d spectra, (b) S 2p spectra, and (c) Cl 2p spectra. Original data (circles) were subtracted using the Shirley background (dashed line) and fitted using the method described in section 2.4. The fitted Pd 3d5/2, Cl 2p3/2, and S 2p3/2 peaks are highlighted (blue and orange) for comparison. The sum of all fitted peaks is shown as a red line.

HCl released or formed would be adsorbed on the stainless steel tubing, preventing its detection.

In the presence of Pd, the TGA plots of as-prepared catalysts clearly depended on the choice of gas (H_2/Ar versus Ar), as shown in Figure 5. The major weight loss of the catalyst prepared using H_2SO_4 shifted 30 °C lower when H_2 was introduced in Ar flow (Figure 5a and c). The volatile products were again similar to those produced from bulk PVA decomposition at 340 °C (Table 4). In addition, MS results indicate H_2 consumption at 160 °C, whereas H_2 production occurred at 320 and 400 °C (Figure 6a, Table 4). H_2 consumption and production was also observed with the sample prepared using HCl (Figure 6b, Table 4). However, the main weight loss was around 310 °C (Figure 5b and d), similar

dx.doi.org/10.1021/cs4004479 | ACS Catal. 2013, 3, 2341−2352

Table 3. Summary of XPS Data on Pd, Cl and S Oxidation States and Surface Concentrations

a. Oxidation States

	Pd $3d_{5/2}$ (eV)		Cl $2p_{3/2}$ (eV)		S $2p_{3/2}$ (eV)	
thermal treatment	Pd^0	Pd^{2+}	Cl (Pd)	Cl (C)	S^{6+}	$S^{\eta-}$ [a]
Pd-PVA/AC_Cl						
	335.7	337.4	198.1	200.6		
H_2/N_2,100 °C	335.6	337.1	198.2	200.7		
H_2/N_2, 200 °C	335.5	337.3	198.1	200.8		
N_2, 200 °C	335.7	337.3	198.0	200.5		
Pd-PVA/AC_S						
	335.7	337.7	198.2	200.7	168.6	
H_2/N_2, 100 °C	335.7	337.1	198.1	200.5	168.6	163.0
H_2/N_2, 200 °C	335.8	337.3			168.3	163.5
H_2/N_2, 250 °C	335.7	337.3			168.4	163.3

b. Relative Molar Concentration

thermal treatment	Pd^{2+}/Pd	Cl (C)/Cl	$S^{\eta-}$/S
Pd-PVA/AC_Cl			
	0.38	0.21	
H_2/N_2,100 °C	0.21	0.37	
H_2/N_2, 200 °C	0.03	0.57	
N_2, 200 °C	0.12	0.50	
Pd-PVA/AC_S			
	0.13	0.15	
H_2/N_2, 100 °C	0.06	0.39	0.22
H_2/N_2, 200 °C	0.03		0.61
H_2/N_2, 250 °C	0.02		0.71

[a] $0 \leq \eta \leq 2$.

to PVA and PVA/AC_Cl (Figure 4d and f). This trend was different as compared with the observations for catalysts prepared with H_2SO_4 (Figure 5a and c), although the volatile compounds detected by MS were again similar (Table 4).

3.7. Catalytic Performance. The catalysts exhibited stable activities on the time scale of hours after initial stabilization time. A typical example of activity as function of time on stream is presented in Supporting Information Figure S2.

3.7.1. Formic Acid Decomposition. The activities of the catalysts for formic acid decomposition at 120 °C, defined per total Pd as well as per surface Pd according to CO chemisorption, are presented in Figure 7a and b. In all experiments, CO_2 and H_2 were the major products. The reaction rate per total Pd for the catalyst prepared using HCl significantly increased after reduction at 200 °C. The same effect was also observed for the catalyst prepared using H_2SO_4, although the resulting activity was only half as compared with the H_2 reduced catalyst prepared using HCl.

The reaction rates per surface Pd were quite similar for the reduced catalysts using either HCl or H_2SO_4 as well as for the as-prepared catalyst prepared using H_2SO_4, as shown in Figure 7b. As-prepared catalyst using HCl showed a higher reaction rate per surface Pd at 120 °C as compared with all other catalysts.

3.7.2. Nitrite Hydrogenation. The activities of the catalysts for nitrite hydrogenation in aqueous phase at 25 °C are also compared, as shown in Figure 7c and d. The reaction rate per total Pd of the catalyst prepared using HCl (Figure 7c) was significantly enhanced after the reduction treatment. In contrast, the reaction rate per total Pd for the catalyst prepared using H_2SO_4 did not show any increase after the reduction treatment.

The activity calculated on the basis of the amount of surface Pd atoms, according to CO chemisorption, strongly decreased as a result of the reduction treatment, independent of the acid used in the catalyst preparation procedure, as shown in Figure 7d.

4. DISCUSSION

4.1. Oxidation and Blocking of the Surface of Pd NPs. Figure 1 and Table 2 show that the Pd particle sizes were identical when either HCl or H_2SO_4 were used to immobilize the colloid for any of the thermal treatments applied. However, it is also shown in Table 2 that the apparent Pd dispersions, according to CO chemisorption, in as-prepared catalysts were significantly lower than the results calculated from TEM. In addition, the catalytic activity per total Pd in as-prepared catalysts was always low, as shown in Figure 7. The obvious explanation is that PVA blocked the surface of Pd NPs, as reported by many other researchers.[3,6,27] Thermal treatment in different atmospheres has often been suggested to remove the capping polymer;[4,28] however, complete removal has been reported to be difficult to achieve, and in any case, a temperature above 300 °C is needed, which easily causes sintering.[9,12] Surprisingly, the data in Table 2 show that it was possible to clean the Pd NPs completely in H_2/N_2 at 200 °C, but only when HCl had been used in the catalyst preparation. In contrast, catalyst prepared with H_2SO_4 could not be cleaned to the same extent. The CO chemisorption data suggest a much lower dispersion as compared with TEM. The effect of the acid on the preparation is therefore discussed in detail below.

Chlorine was present in all catalysts, independently of the acid used during colloid immobilization, as shown in Table 2 and confirmed by XPS (Figure 3c). It is known that the presence of chlorine in Pd catalysts decreases the capacity of CO chemisorption;[29] therefore, it is difficult to discern whether the low CO adsorption capacity was due to the presence of Cl or the PVA blocking effect. The presence of a small content of chlorine in as-prepared catalyst using H_2SO_4 originated from the Pd precursor, Na_2PdCl_4. It is well-known that complete removal of Cl from Pd catalyst prepared with Cl containing precursors is difficult via reduction by $NaBH_4$ or even by treatment in H_2 below 100 °C.[30−32] Therefore, the presence of Cl on Pd may well contribute to the extremely low CO chemisorption capacity in as-prepared catalysts, as shown in Table 2.

When HCl was used instead of H_2SO_4 during colloid immobilization, the chlorine content as well as the fraction of oxidized Pd tripled in the as-prepared catalyst, indicating a strong correlation between the chlorine content and the Pd oxidation state. Obviously, the additional chlorine was introduced by HCl. The immobilization was always performed in the presence of air. We suggest that the presence of HCl enhanced the oxidation of the Pd NPs with O_2, according to the following reaction equations:

$$2Pd + O_2 \rightarrow 2PdO \quad \Delta G = -186.82\ kJ \tag{3}$$

$$PdO + 2Cl^- + 2H^+ \rightarrow PdCl_2 + H_2O(l) \quad \Delta G = -41.38\ kJ \tag{4}$$

The resulting overall reaction is

dx.doi.org/10.1021/cs4004479 | ACS Catal. 2013, 3, 2341−2352

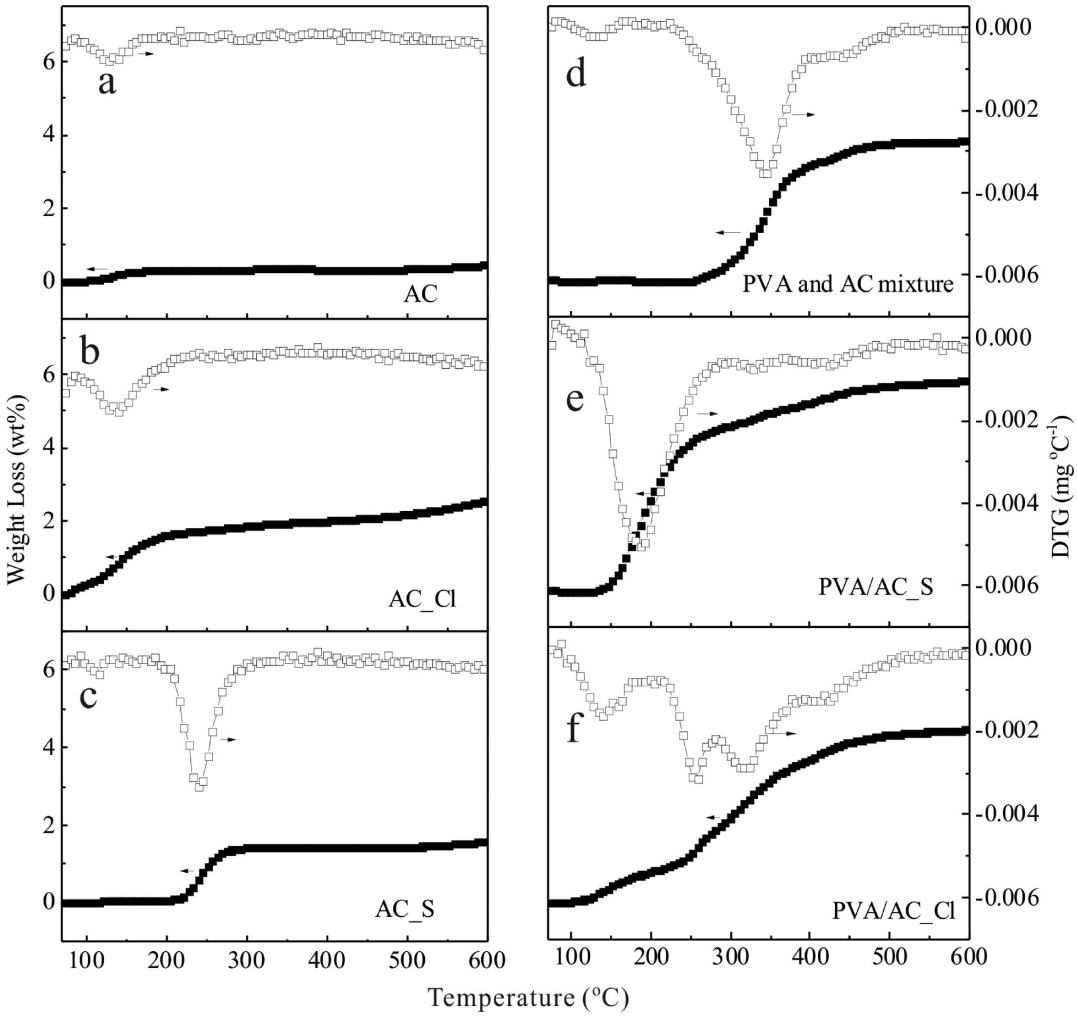

Figure 4. TGA-DTG in Ar atmosphere: (a) activated carbon, (b) activated carbon treated in HCl at pH = 2, (c) activated carbon treated in H_2SO_4 at pH = 2, (d) PVA and AC mechanical mixture, (e) PVA/AC_S, and (f) PVA/AC_Cl.

$$2Pd + Cl^- + O_2 + 4H^+ \rightarrow 2PdCl_2 + 2H_2O(l)$$
$$\Delta G = -269.57\ kJ \quad (5)$$

According to the XPS results in Table 3, 36% of Pd was oxidized when using HCl, and this percentage was quite similar to the Pd dispersion observed by TEM (38%, Table 2). This would indicate that the surface of the Pd NPs was completely oxidized with Cl^- as the counterion.

UV−vis spectra of unsupported colloid (Supporting Information Figure S1) indicate reoxidation and redissolution of Pd NPs in the presence of O_2 and Cl^-. On the other hand, the Pd particle sizes (TEM in Figure 1) and Pd contents (XRF results in Table 1) show no difference for AC-supported catalysts, regardless which acid was used. Thus, the redissolution of Pd during colloid immobilization was only a minor effect.

As shown by XRF (Table 2) and XPS (Figure 3, Table 3), chlorine bonded to Pd was removed by the reduction in H_2/N_2, especially at higher temperature, suggesting that $PdCl_x$ was converted to Pd^0 and HCl. The Pd dispersion calculated on the basis of the CO chemisorption was comparable with TEM observations after reduction at 200 °C in H_2/N_2, indicating that complete exposure of the Pd surface was obtained.

Given the fact that Cl^- interacted significantly with the Pd NPs, we propose that the presence of Cl^- and O_2 during colloid immobilization weakens the interaction between Pd NPs and PVA, explaining why PVA was found to be completely removed by H_2 treatment at 200 °C. This proposition is schematically presented in Figure 8.

On the other hand, when H_2SO_4 was used, 13% of the Pd was present as Pd^{2+} in the as-prepared catalyst, as shown in Table 3. The oxidized Pd could be reduced almost completely in H_2/N_2 because only 2% of Pd atoms remained oxidized after reduction at 250 °C. However, the Pd surface area accessible for CO chemisorption was still very low as compared with the particle size, according to TEM. Therefore, the limited accessibility of the surface of the Pd NPs was caused by other factors. Before concluding that blocking by PVA is responsible, two alternative explanations will be discussed shortly.

Because the mean diameter of the Pd NPs in all catalysts was >2 nm, most of the Pd NPs should be located in mesopores. As shown in Figure 2, no blocking of mesopores was observed, according to N_2 physisorption results, indicating that PVA did not decrease the accessibility of those pores containing Pd NPs.

Another alternative explanation might be the presence of S in the catalysts prepared with H_2SO_4, because S poisoning of Pd is a well-known phenomenon.[33−35] As shown in Table 2, almost

dx.doi.org/10.1021/cs4004479 | ACS Catal. 2013, 3, 2341−2352

Table 4. Summary of TGA-DTG Results

sample	atmosphere	wt loss at 200 °C (wt%)	wt loss position: peak range (°C)	wt loss position: peak position (°C)	related gas products according to MS
AC	H_2/Ar	0.35	90−160	120	H_2O
	Ar	0.34	90−160	120	H_2O
AC_Cl	H_2/Ar	1.58	90−190	130	
	Ar	1.62	90−190	130	
AC_S	H_2/Ar	0.04	210−280	240	
	Ar	0.05	210−280	240	
PVA and AC mechanical mixture	H_2/ Ar	0.10	250−450	120	H_2O
				340	H_2O, CO_2, $-CH_3$
				400	$-CH_3$
	Ar	0.08	250−450	120	H_2O
				340	H_2O, CO_2, $-CH_3$
PVA-AC_S	H_2/ Ar	2.91	120−300	190	H_2O, CO_2, $-CH_3$
	Ar	2.88	120−300	190	H_2O, CO_2, $-CH_3$
PVA-AC_Cl	H_2/ Ar	0.82	220−450	120	H_2O
				250	H_2O, CO_2, $-CH_3$
				315	H_2O, CO_2, $-CH_3$
				400	$-CH_3$
	Ar	0.84	220−450	120	H_2O
				250	H_2O, CO_2, $-CH_3$
				315	H_2O, CO_2, $-CH_3$
				400	$-CH_3$
Pd-PVA/ AC_S	H_2/ Ar	2.38	90−450	160	H_2 (negative), H_2O, CO_2, and $-CH_3$
				320	H_2, H_2O, CO_2, $-CH_3$
				400	H_2, $-CH_3$
	Ar	2.26	130−450	190	H_2O, CO_2, −CH3
				315	H_2O, CO_2, $-CH_3$
				400	H_2, $-CH_3$
Pd-PVA/ AC_Cl	H_2/ Ar	1.47	90−400	155	H_2 (negative), H_2O, CO_2
				315	H_2, H_2O, $-CH_3$
				400	H_2, $-CH_3$
	Ar	0.48	90−400	310	H_2O, CO_2, $-CH_3$
				400	H_2, $-CH_3$

all sulfur species originated from H_2SO_4. Reduction of S^{6+} species to S^0/S^{2-} species was observed (Figure 3b), accompanied by reduction of Pd^{2+} as well as an increase in the apparent Pd dispersion according to CO chemisorption, as shown in Tables 2 and 3. Both of these observations illustrate that the formation of S^0/S^{2-} is not accompanied by formation of PdS on the surface of the Pd particles. Insignificant interaction of the S species with Pd is also illustrated by the fact that the S content in Pd-PVA/AC_S was even lower than in PVA/AC_S.

In summary, PVA blocked the Pd surface of the nanoparticles in the catalyst prepared using H_2SO_4 during colloid immobilization. When HCl was used instead, PVA coverage was suppressed by Cl bonded to Pd, whereas Cl was removed by reduction in H_2/N_2, resulting in a clean surface of Pd NPs.

4.2. PVA Thermal Stability. As shown in Figure 4, the choice of acid used for colloid immobilization also influenced the thermal stability of PVA in inert atmosphere. In the presence of H_2SO_4, the decomposition temperature of PVA dispersed on AC (Figure 4e) was 150 °C lower as compared with PVA in the mechanical mixture (Figure 4d). Three reasons can be suggested to explain this: First, PVA decomposition might be promoted catalytically by sulfonic acid on AC or PVA, in a way similar to the catalytic decomposition of cross-linked PVA by sulfosuccinic acid (SSA) in the study of Morancho et al.[36] Second, Yang et al. demonstrated decreasing thermal stability when hydrolyzing PVA.[25] The PVA used in this study was produced from polyvinyl acetate[37] and was hydrolyzed to 87−89% as purchased. It is quite possible that further hydrolysis of PVA occurred in the presence of H_2SO_4 in the aqueous phase, thus decreasing the thermal stability. Finally, third, PVA was possibly well dispersed on the AC surface, thus increasing the surface area of PVA, which was likely to enhance its thermal decomposition. Further research would be necessary to see distinctions among these three options.

In contrast, the TGA results of PVA dispersed on AC prepared with HCl (Figure 4f) indicate a much milder effect on promoting PVA decomposition as compared with H_2SO_4. Comparing with the TGA result of PVA in the mechanical mixture (Figure 4d), the new weight-loss step around 250 °C would indicate a lesser influence of the possible reasons discussed above.

Remarkably, PVA decomposition in inert atmosphere was not influenced by the presence of Pd (comparing Figure 4e and 5c as well as Figure 4f and 5d). This indicates that PVA was mainly dispersed on the AC, and the interaction with Pd involved only a minor fraction of the PVA in the catalyst. However, in H_2/Ar, the presence of Pd caused an additional weight-loss step that appeared around 160 °C (Figure 5b and d), concurrently with hydrogen consumption and H_2O production (Figure 6), indicating hydrogenolysis of PVA catalyzed by Pd NPs according to the following reaction:

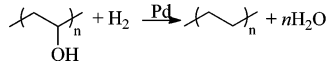

(6)

The catalyst prepared using H_2SO_4 exhibited a more significant weight loss (for both decomposition and hydrogenation) compared with the catalyst prepared using HCl at 200 °C (Table 4). However, the capacity for CO chemisorption did not increase (Table 2). This indicates again that the majority of the PVA interacted with AC, whereas only a minor fraction was involved in the interaction with Pd NPs, decreasing the accessible Pd surface area.

4.3. Catalytic Activity. *4.3.1. Activity per Total Pd.* The influence of the choice of acid and thermal treatment on the catalyst performance was studied with the reactants in the gas phase vs reactants in the aqueous phase using formic acid decomposition and nitrite hydrogenation as model reactions, respectively.

In both reactions, treatment at 200 °C in H_2/N_2 increased the reaction rate per total Pd for the catalyst prepared using HCl, as shown in Figure 7a and c, together with increasing apparent Pd dispersion calculated from CO chemisorption in Table 2, as well as further reduction of Pd and removal of Cl

dx.doi.org/10.1021/cs4004479 | ACS Catal. 2013, 3, 2341−2352

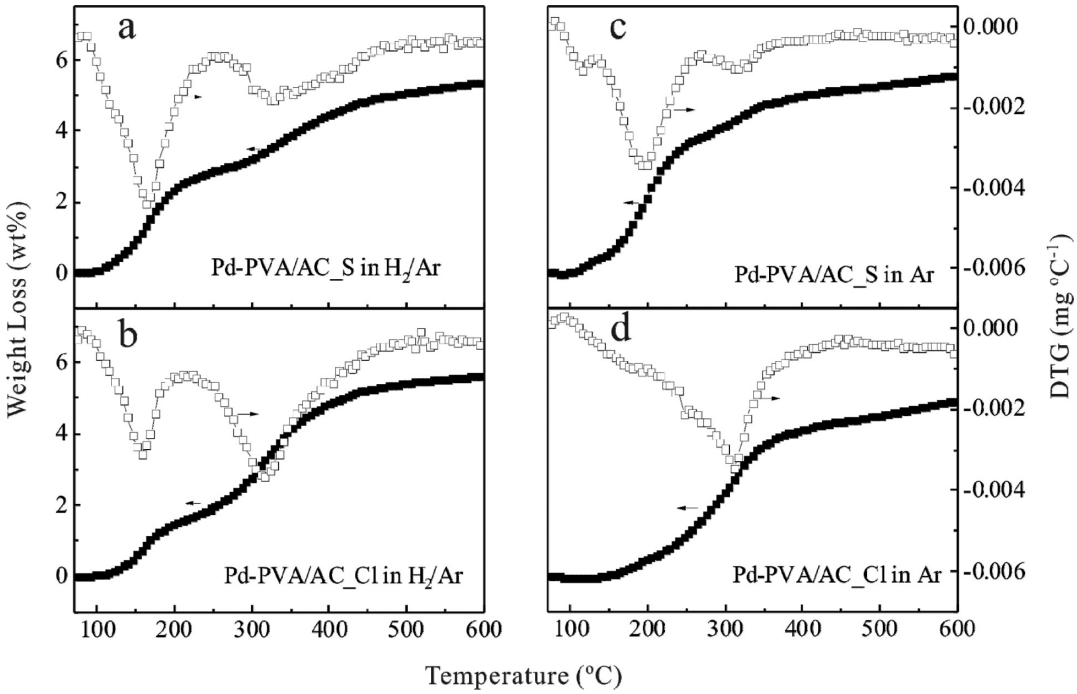

Figure 5. Weight loss and DTG of sample containing PVA in H_2/Ar (left) and Ar (right) atmosphere.

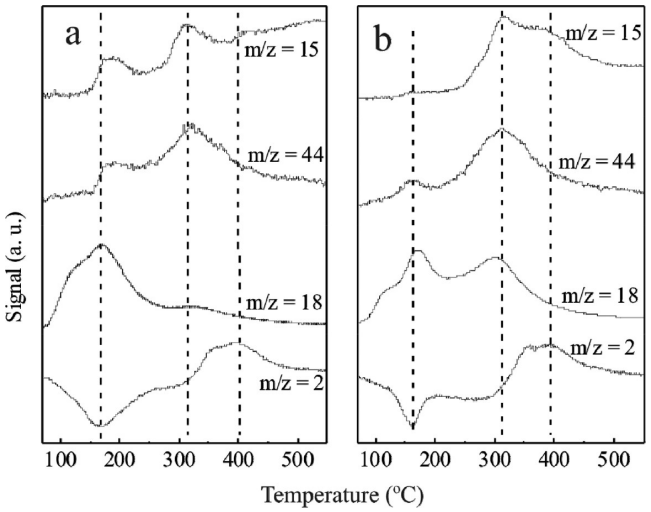

Figure 6. Trends in selected m/z values as detected with MS downstream during H_2-TPR of (a) Pd-PVA/AC_S and (b) Pd-PVA/AC_Cl. Gas composition, 5% H_2/95% Ar. Heating rate, 5 °C min^{-1}.

bonded to Pd as observed by XPS in Table 3. As discussed above, this confirms that the thermal treatment in H_2/N_2 together with the use of HCl increased the accessibility of surface Pd atoms on the nanoparticles, enhancing the activity for both reactions.

However, catalysts prepared with H_2SO_4 revealed very different effects on the activity in the two reactions after treatment in H_2/N_2. The activity for nitrite hydrogenation decreased slightly after reduction in H_2/N_2 at 200 °C (Figure 7c), whereas activity for formic acid decomposition increased strongly (Figure 7a). All catalysts prepared with H_2SO_4 were much less active as compared with the reduced catalysts prepared using HCl, which can be attributed to the remaining capping agent on the Pd NPs. As aforementioned, TGA results (Figure 5a) indicate that PVA mostly decomposed at 200 °C in H_2/Ar; thus, a minor fraction of PVA in the catalysts is responsible for the partial deactivation of the Pd surface.

4.3.2. Activity per Surface Pd. Figure 7b shows that the activity per Pd surface atom for formic acid decomposition varied only slightly for all catalysts. Thus, the activity scales with the number of sites accessible for CO. Note that CO chemisorption for as-prepared catalyst prepared using HCl was performed after a pretreatment including reduction at room temperature. Possibly Pd was partially reduced by formic acid during the reaction, increasing the actual number of Pd surface active sites as compared with the estimation based on CO chemisorption.

In the case of nitrite hydrogenation in the aqueous environment, the activity per surface Pd atom varied significantly after the thermal treatment in H_2/N_2. For the catalyst prepared using HCl, this was probably an artifact: the as-prepared catalyst contained an extremely high chlorine concentration, causing a low CO chemisorption capacity. Probably, part of the chlorine was removed by H_2 during the nitrite hydrogenation, which is supported by the fact that Cl^- was detected in the product liquid initially. As a consequence, the number of Pd surface sites was underestimated, and the activity per Pd surface atom was overestimated.

By comparison, the catalyst prepared using H_2SO_4 showed even more significant decrease in activity per Pd surface atom after reduction in H_2/N_2 at 200 °C, as shown in Figure 7d. Increasing the number of active sites during the reaction was not likely to be the main reason in this case because the catalyst contained much less chlorine as well as oxidized Pd (Table 3). Therefore, it is proposed that the main reason was the effect of the reaction medium (gas vs water) on the arrangement of the PVA molecules on the surface of the Pd NPs. Because PVA has a high affinity for water, it is expected that PVA will cover the Pd surface more extensively when exposed to the gas phase (during CO chemisorption), whereas in aqueous medium (during nitrite hydrogenation), the PVA molecules tend to interact with water, decreasing the coverage of the Pd surface.

dx.doi.org/10.1021/cs4004479 | ACS Catal. 2013, 3, 2341−2352

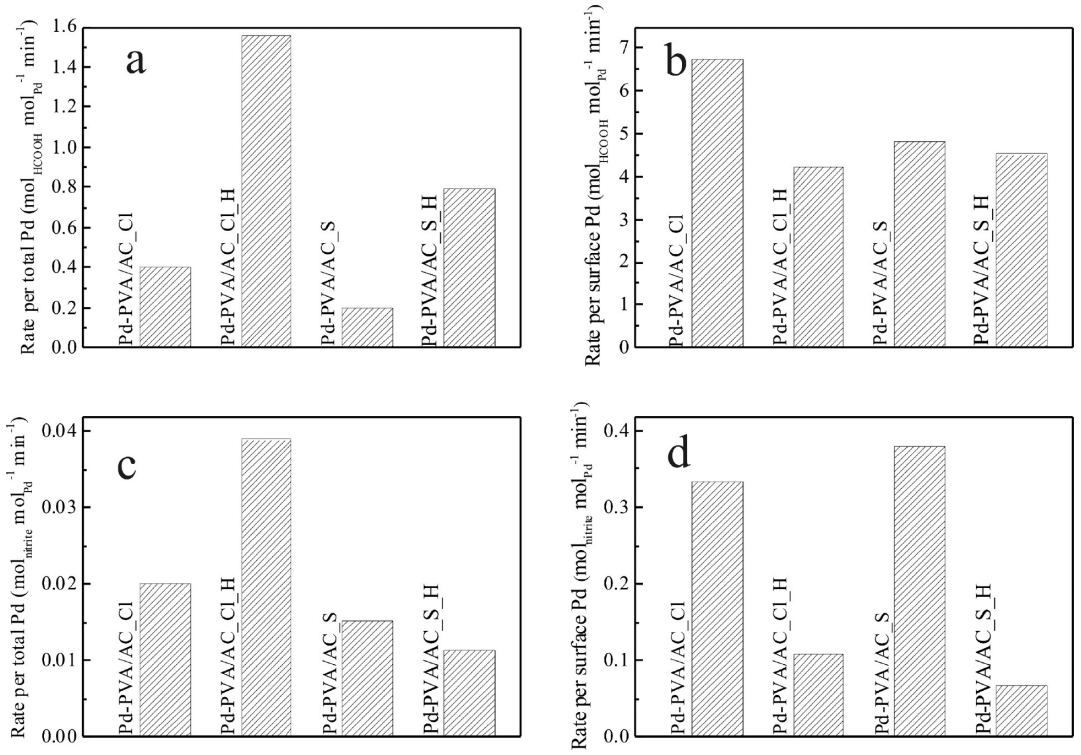

Figure 7. Reaction rate (a) per total Pd and (b) per surface Pd determined by CO chemisorption for formic acid catalytic decomposition at 120 °C, and reaction rate (c) per total Pd and (d) per surface Pd determined by CO chemisorption for nitrite hydrogenation at 25 °C.

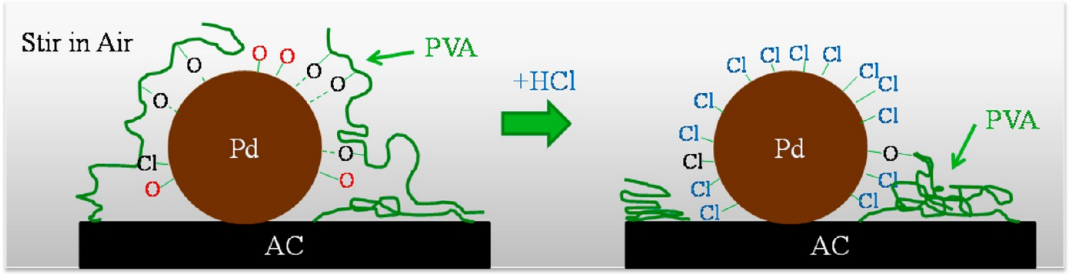

Figure 8. Proposed mechanism of chlorine suppressing PVA coverage on Pd NPs.

Consequently, the number of Pd atoms accessible on the surface in water was probably underestimated by CO chemisorption, resulting in an overestimated activity per surface Pd for catalyst prepared using H_2SO_4.

5. CONCLUSIONS

The choice of acid during Pd colloid immobilization on activated carbon is critical to achieving complete accessibility of surface Pd atoms. Usage of HCl efficiently suppresses blocking of the surface of the immobilized Pd NPs by PVA. Clean and catalytically active Pd NPs can be achieved after reduction in H_2/N_2 atmosphere at 200 °C without any significant sintering.

In contrast, H_2SO_4 does not induce this suppressing effect, and PVA continues to block a significant part of the Pd surface. The extent of blocking of the Pd surface by PVA is less significant in water as compared with in the gas phase, which is addressed to the interaction of PVA with water, partially suppressing the interaction with the metal surface. This is reflected in the catalytic activity for formic acid decomposition in the gas phase versus nitrite hydrogenation in the aqueous phase.

The majority of the PVA molecules interact with only the support and the temperature of PVA decomposition is therefore not a useful parameter for developing methods to obtain clean Pd NPs.

■ ASSOCIATED CONTENT

Ⓢ Supporting Information

Additional experimental details and results as noted in text. This material is available free of charge via the Internet at http://pubs.acs.org.

■ AUTHOR INFORMATION

Corresponding Author

*E-mail: L.Lefferts@utwente.nl.

Notes

The authors declare no competing financial interest.

■ ACKNOWLEDGMENTS

The authors greatly acknowledge Norit for supplying activated carbon. We are highly grateful to the constructive suggestions of Prof. Yongdan Li from Tianjin University, China. We are

also grateful to M. Smithers for TEM, G. A. M. Kip for XPS, J. A. M. Vrielink for BET and XRF measurements, and K. Altena-Schildkamp for CO chemisorption measurements. We acknowledge Ing. B. Geerdink for technical support.

REFERENCES

(1) Xia, Y.; Xiong, Y.; Lim, B.; Skrabalak, S. E. *Angew. Chem., Int. Ed.* **2009**, *48* (1), 60−103.
(2) Semagina, N.; Kiwi-Minsker, L. *Catal. Rev.* **2009**, *51* (2), 147−217.
(3) Villa, A.; Wang, D.; Su, D. S.; Prati, L. *ChemCatChem* **2009**, *1* (4), 510−514.
(4) Rodrigues, E. G.; Carabineiro, S. A. C.; Delgado, J. J.; Chen, X.; Pereira, M. F. R.; Órfão, J. J. M. *J. Catal.* **2012**, *285* (1), 83−91.
(5) Gaikwad, A. V. *Nanocatalysts: Properties and Applications*; Ph.D. Thesis, University of Amsterdam, Amsterdam, 2009.
(6) Quintanilla, A.; Butselaar-Orthlieb, V. C. L.; Kwakernaak, C.; Sloof, W. G.; Kreutzer, M. T.; Kapteijn, F. *J. Catal.* **2010**, *271* (1), 104−114.
(7) Wang, X.; Sonström, P.; Arndt, D.; Stöver, J.; Zielasek, V.; Borchert, H.; Thiel, K.; Al-Shamery, K.; Bäumer, M. *J. Catal.* **2011**, *278* (1), 143−152.
(8) Aliaga, C.; Park, J. Y.; Yamada, Y.; Lee, H. S.; Tsung, C.-K.; Yang, P.; Somorjai, G. A. *J. Phys. Chem. C* **2009**, *113* (15), 6150−6155.
(9) Borodko, Y.; Lee, H. S.; Joo, S. H.; Zhang, Y.; Somorjai, G. *J. Phys. Chem. C* **2009**, *114* (2), 1117−1126.
(10) Rioux, R. M.; Song, H.; Hoefelmeyer, J. D.; Yang, P.; Somorjai, G. A. *J. Phys. Chem. B* **2004**, *109* (6), 2192−2202.
(11) Dash, P.; Bond, T.; Fowler, C.; Hou, W.; Coombs, N.; Scott, R. W. J. *J. Phys. Chem. C* **2009**, *113* (29), 12719−12730.
(12) Baker, L. R.; Kennedy, G.; Krier, J.; Spronsen, M.; Onorato, R.; Somorjai, G. *Catal. Lett.* **2012**, *142* (11), 1286−1294.
(13) Lopez-Sanchez, J. A.; Dimitratos, N.; Hammond, C.; Brett, G. L.; Kesavan, L.; White, S.; Miedziak, P.; Tiruvalam, R.; Jenkins, R. L.; Carley, A. F.; Knight, D.; Kiely, C. J.; Hutchings, G. J. *Nat. Chem.* **2011**, *3* (7), 551−556.
(14) Lin, S. D.; Hsu, Y.-H.; Jen, P.-H.; Lee, J.-F. *J. Mol. Catal. A: Chem.* **2005**, *238* (1−2), 88−95.
(15) Villa, A.; Wang, D.; Dimitratos, N.; Su, D.; Trevisan, V.; Pratia, L. *Catal. Today* **2010**, *150* (1−2), 8.
(16) Rouquerol, F.; Rouquerol, J.; Sing, K. Adsorption by Active Carbons. *Adsorption by Powders and Porous Solids*; Academic Press: London, 1999; pp 237−285.
(17) Briggs, D.; Grant, J. T. *Surface Analysis by Auger and X-Ray Photoelectron Spectroscopy*; IM Publications: Chichester, 2003.
(18) Moulder, J. F.; Stickle, W. F.; Sobol, P. E.; Bomben, K. D. *Handbook of X-ray Photoelectron Spectroscopy*; Perkin-Elmer Corporation: Eden Prairie, MN, 1992.
(19) Bulushev, D. A.; Jia, L.; Beloshapkin, S.; Ross, J. R. H. *Chem. Commun.* **2012**, *48* (35), 4184−4186.
(20) Amorim, C.; Yuan, G.; Patterson, P. M.; Keane, M. A. *J. Catal.* **2005**, *234* (2), 268−281.
(21) Pinna, F.; Menegazzo, F.; Signoretto, M.; Canton, P.; Fagherazzi, G.; Pernicone, N. *Appl. Catal., A* **2001**, *219* (1−2), 195−200.
(22) Simonov, P. A.; Romanenko, A. V.; Prosvirin, I. P.; Moroz, E. M.; Boronin, A. I.; Chuvilin, A. L.; Likholobov, V. A. *Carbon* **1997**, *35* (1), 73−82.
(23) Naumkin, A. V.; Kraut-Vass, A.; Gaarenstroom, S. W.; Powell, C. J. *NIST X-ray Photoelectron Spectroscopy Database*; http://srdata.nist.gov/xps/Default.aspx (accessed September 15, 2012).
(24) Cai, J. H.; Morris, E.; Jia, C. Q. *J. Sulfur Chem.* **2009**, *30* (6), 555−569.
(25) Yang, H.; Xu, S.; Jiang, L.; Dan, Y. *J. Macromol. Sci., Part B: Phys.* **2011**, *51* (3), 464−480.
(26) Thomas, P.; Guerbois, J. P.; Russell, G.; Briscoe, B. *J. Therm. Anal. Calorim.* **2001**, *64* (2), 501−508.
(27) Chinthaginjala, J. K.; Villa, A.; Su, D. S.; Mojet, B. L.; Lefferts, L. *Catal. Today* **2012**, *183* (1), 119−123.
(28) Okhlopkova, L.; Kerzhentsev, M.; Tuzikov, F.; Larichev, Y.; Ismagilov, Z. *J. Nanopart. Res.* **2012**, *14* (9), 1−15.
(29) Sepúlveda, J.; Fígoli, N. *React. Kinet. Catal. Lett.* **1994**, *53* (1), 155−160.
(30) Zharmagambetova, A. K.; Golodov, V. A.; Saltykov, Y. P. *J. Mol. Catal.* **1989**, *55* (1), 406−414.
(31) Zharmagambetova, A. K.; Mukhamedzhanova, S. G.; Bekturov, E. A. *React. Polym.* **1994**, *24* (1), 17−20.
(32) Badano, J. M.; Quiroga, M.; Betti, C.; Vera, C.; Canavese, S.; Coloma-Pascual, F. *Catal. Lett.* **2010**, *137* (1−2), 35−44.
(33) Marshall, S. T.; Medlin, J. W. *Surf. Sci. Rep.* **2011**, *66* (5), 173−184.
(34) Gravil, P. A.; Toulhoat, H. *Surf. Sci.* **1999**, *430* (1−3), 176−191.
(35) Gan, L.-Y.; Zhang, Y.-X.; Zhao, Y.-J. *J. Phys. Chem. C* **2009**, *114* (2), 996−1003.
(36) Morancho, J. M.; Salla, J. M.; Cadenato, A.; Fernández-Francos, X.; Ramis, X.; Colomer, P.; Calventus, Y.; Ruíz, R. *Thermochim. Acta* **2011**, *521* (1−2), 139−147.
(37) Tamaki, R.; Chujo, Y. *Appl. Organomet. Chem.* **1998**, *12* (10−11), 755−762.